JOURNAL OF THERMOPHYSICS AND HEAT TRANSFER
Vol. 9, No. 3, July–September 1995

Analytical Method for Forced Convection from Flat Plates, Circular Cylinders, and Spheres

G. Refai Ahmed* and M. M. Yovanovich†
University of Waterloo, Waterloo, Ontario N2L 3G1, Canada

A simple general method is developed to predict forced convection heat transfer from isothermal body shapes such as flat plates, infinite circular cylinders, and spheres for a wide range of both Reynolds number and Prandtl number. The proposed method is based on linearization of the thermal energy equation that is accomplished by the introduction of an effective velocity that is related to the freestream velocity. Next, the linear energy equation is transformed to an equivalent transient heat conduction equation that has existing solutions. These solutions are retransformed to the final expression as a function of the effective velocity that is defined in the limits of $Pr \to \infty$ and $Pr \to 0$ using scaling analysis. The approximate analytic solutions are in closed form, they are simple and quite accurate when compared with previous experimental and analytical studies.

Nomenclature

A = surface area, m^2
C_D = constant in Table 1
C_j = constant in Eq. (2)
C_0 = constant in Eq. (16)
D = sphere or cylinder diameter, m
$F(Pr, \gamma_j)$ = function defined in Eq. (3)
Fo_j = Fourier number, $\alpha t/\mathscr{L}^2$
h = coefficient of convection heat transfer, W/m^{2}K
$\hbar_1, \hbar_2, \hbar_3$ = curvilinear scale factors
i = notation index
$ierfc$ = first integral of complementary error function
i^2erfc = second integral of complementary error function
k = thermal conductivity, W/m K
L = flat plate and cylinder length, m
$\mathscr{L}$ = arbitrary scale length, m
Nu_j = area-averaged Nusselt number, $\mathscr{L}h/k$
Nu_j^0 = area-averaged Nusselt number at the diffusive limit
Pe_j = Peclet number, $\mathscr{L}V_\infty/\alpha$
Pr = Prandtl number, ν/α
Q = total heat flow rate, W
q = heat flux, W/m^2
q_S = heat flux at the surface, W/m^2
Re_j = Reynolds number, $\mathscr{L}V_\infty/\nu$
$Re_j(\theta)$ = local Reynolds number, $\mathscr{L}V(\theta)/\nu$
r, θ, Z = cylindrical coordinates
r, θ, ϕ = spherical coordinates
T = temperature, K
T^* = nondimensional temperature, $(T - T_\infty)/(T_S - T_\infty)$
T_S = surface temperature, K
T_∞ = ambient temperature, K
t = time, s
u_1, u_2, u_3 = velocities in curvilinear coordinates, m/s
V = local velocity at the edge of thermal boundary layer, m/s
$V(\theta)$ = local velocity at the edge of hydrodynamic boundary layer, m/s
V_∞ = freestream velocity, m/s
$\bar{v}_e$ = area-averaged effective velocity, m/s
$\bar{v}_e^\infty$ = area-averaged effective velocity as $Pr \to \infty$, m/s
$\bar{v}_e^0$ = area-averaged effective velocity as $Pr \to 0$, m/s
$\bar{v}_e^\infty(\theta)$ = local effective velocity as $Pr \to \infty$, m/s
W = flat plate width, m
X, Y, Z = Cartesian coordinates
x_1, x_2, x_3 = curvilinear coordinates
α = thermal diffusivity, $k/C_p\rho$, m^2/s
γ = parameter in Eq. (18)
δ = local thickness of hydrodynamic boundary layer, m
δ_{i2} = Kronecker delta in x_2 direction
δ_T = local thickness of thermal boundary layer, m
δ_D^T = displacement thickness of thermal boundary layer, m
δ_M^T = momentum thickness of thermal boundary layer, m
η = nondimensional quantity, y/δ
ν = kinematic viscosity, m^2/s
ρ = mass density, kg/m^3

Received March 30, 1994; presented as Paper 94-1971 at the AIAA/ASME 6th Joint Thermophysics and Heat Transfer Conference, Colorado Springs, CO, June 20–23, 1994; revision received Dec. 6, 1994; accepted for publication Dec. 8, 1994. Copyright © 1995 by G. R. Ahmed and M. M. Yovanovich. Published by the American Institute of Aeronautics and Astronautics, Inc., with permission.

*Research Assistant, Department of Mechanical Engineering, Microelectronics Heat Transfer Laboratory. Senior Member AIAA.

†Professor and Director, Department of Mechanical Engineering, Microelectronics Heat Transfer Laboratory. Fellow AIAA.

Introduction

EXTERNAL forced convection heat transfer from isothermal or isoflux external convex surfaces is an important problem for engineers. There are many engineering systems that are modeled using forced convection, such as electronic components on printed circuit boards placed in cabinets, hot wire anemometer, and heat exchanger design.

A schematic of the different body shapes, which are investigated in this study, is shown in Fig. 1. These different body shapes are maintained at T_S and the environment is maintained at T_∞. These bodies are subjected to a uniform steady flow.

The present study is concerned with the effects of Reynolds number, Prandtl number, and velocity profiles on forced convection heat transfer from isothermal surfaces such as flat plates (FP), infinite circular cylinders (ICC) and spheres.

Literature Survey

The objective of this section is to present a brief summary of some previous studies dealing with external forced con-

Table 1 Recalculation of the Hilpert[10] air data by Morgan,[9] $Nu_D = C_D Re_D^m$

		Hilpert[10]		Morgan[9]	
Re_D	L/D	C_D	m	C_D	m
1–4	5,120	0.891	0.33	—	—
4–40	1,625–5,120	0.821	0.385	0.795	0.384
40–4,000	20–3,170	0.615	0.466	0.583	0.471
4,000–40,000	5.6–20	0.174	0.618	0.148	0.633
40,000–400,000	0.9–11.4	0.0239	0.805	0.0208	0.814

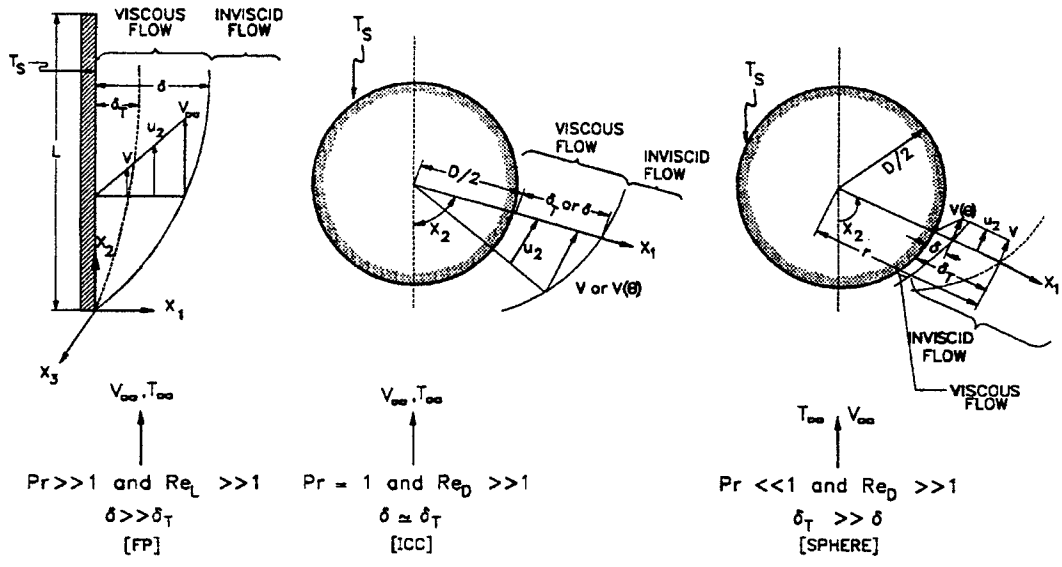

Fig. 1 Schematic diagram of boundary layers over different body shapes.

vection heat transfer from flat plates, infinite circular cylinders, and spheres. This summary will also show limitations in the previous investigations and their discrepancies.

Flat Plates

Forced convection from isothermal flat plates has been investigated since the beginning of this century and different solutions have been developed for specific ranges of Pr and Re_l. In addition, other investigations have been done to provide better understanding of the problem such as the recent study of Yovanovich et al.[1] However, the effect of velocity profiles as a function of Reynolds number on the heat transfer results has not been investigated in previous studies such as Pohlhausen (see Kays and Crawford[2]), Schlichting,[3] and Yovanovich et al.[1] Furthermore, there are disagreements between experimental studies and analytical studies such as the investigations of Slegel and Hawkins,[4] Parmalee and Huebscher,[5] and Knudsen and Katz.[6]

Circular Cylinders

Numerous studies have been done to correlate heat transfer by forced convection from circular cylinders in crossflow in the following form: $Nu_l = Nu_l(Re_l, Pr)$. However, all of them have failed to establish a general form: $Nu_l = Nu_l(L/D, Re_l, Pr)$. In addition, there are many two-dimensional numerical studies,[7] however, the L/D is not defined. Furthermore, Churchill and Bernstein[8] developed a general correlation for forced convection heat transfer from horizontal circular cylinders to cover a wide range of Reynolds number:

$$Nu_D = 0.3 + \left\{0.62 Re_D^{0.5} \frac{Pr^{1/3}}{[1 + (0.4/Pr)^{2/3}]^{1/4}} \cdot [1 + (Re_D/282{,}000)^{5/8}]^{4/5}\right\} \quad (1)$$

for $10^2 \leq Re_D \leq 10^7$.

Equation (1) has been developed for infinite circular cylinder, i.e., $L >> D$ based on fitting many experimental data from the literature.

Morgan[9] presented a comprehensive literature review for this problem and developed various correlations for the crossflow over cylinders based on the experimental data of Hilpert[10] as shown in Table 1. One observes from Table 1 that the Morgan correlations are valid for specific values of L/D and also specific ranges of Reynolds number.

Spheres

Steady forced convection heat transfer from isothermal spheres into a substantial amount of fluid has been investigated experimentally, theoretically, and numerically by many researchers.[11]

The effects of Pr, Re_D, and velocity profiles on forced convection heat transfer have also been investigated for this case by Refai Ahmed and Yovanovich[11] using an approximate analytical method.

Remarks

Exact solutions for forced convection heat transfer from arbitrary body shapes are very difficult to obtain, since the governing equations dealing with this type of problem are nonlinear. Furthermore, the researchers, who investigated this problem analytically, developed their solutions for specific ranges of Prandtl and Reynolds numbers. The difficulties of predicting forced convection heat transfer are summarized as follows:

1) Starting with the full governing equations creates difficulties to the analytical solution due to the nonlinear equations and the pressure change over arbitrary body shapes. In addition, consideration of flow separation over the body shapes precludes any further analysis of the governing equations.

2) Numerical techniques are expensive and also require large computational effort.

3) Experimental techniques are time-consuming, expensive, and test specific.

Objectives

In the present investigation an approximate analytical study will be conducted to determine the effect of various parameters upon the area-averaged Nusselt number. One of the important goals of the present study is to consider the effects of Reynolds number, Prandtl number, and velocity profiles on the area-averaged Nusselt number. Also, a general model for forced convection heat transfer from flat plates, infinite circular cylinders, and spheres will be developed in the following form:

$$Nu_f = Nu_f^0 + C_f\sqrt{Re_f}F(Pr, \gamma_f) \tag{2}$$

where Nu_f^0 is the area-averaged Nusselt number at the diffusive limit, C_f is a constant that depends on the body shape, and $F(Pr, \gamma_f)$ is a function that depends on fluid properties and velocity profiles through the parameter γ_f, where γ_f is a function of Reynolds number.

Theoretical Analysis

The proposed approximate analytical method can be outlined as follows: one must convert the energy equation to a linear partial differential equation; furthermore, the new linear partial differential equation can be transformed to a transient equation in order to obtain the final form of Nu_f as a function of area-mean effective velocity $\bar{v}_e$; the next step is to examine the governing equations using scaling analysis for $Re_f >> 1$ and $Pr >> 1$, and $Re_f >> 1$ and $Pr << 1$ in order to determine $\bar{v}_e$; this is accomplished by applying scaling analysis inside the hydrodynamic boundary layer for both the continuity and momentum equations to obtain $\delta/\mathscr{L}$; in addition, one must apply scaling analysis inside the thermal boundary layer for both the continuity and energy equations in order to obtain $\delta_T/\mathscr{L}$; one can define $\bar{v}_e^\infty$ through momentum balances inside the thermal boundary layer; by contrast, one can obtain from the right side of the flow chart the definition of $\bar{v}_e^0$, which presents the case of $Pr << 1$ and $Re_f >> 1$, by applying boundary-layer concepts; and finally, one applies a "blending" method in order to find $\bar{v}_e$ for all Prandtl numbers and then substitute it in the Nusselt number to obtain the final expression.

Figure 1 shows an isothermal FP, ICC, and sphere of temperature T_S and length L for the FP, and diameter D for both the ICC and the sphere, which are immersed in a steady, laminar, and incompressible flow of a constant property fluid ($0 < Pr < \infty$) at constant temperature T_∞ and uniform upstream velocity V_∞. In addition, Fig. 1 describes the hydrodynamic and thermal boundary layers for various Prandtl numbers at $Re_f >> 1$. The energy equation with negligible heat dissipation in orthogonal curvilinear coordinates is

$$\left[\frac{u_1}{\hbar_1}\frac{\partial T}{\partial x_1} + \frac{u_2}{\hbar_2}\frac{\partial T}{\partial x_2} + \frac{u_3}{\hbar_3}\frac{\partial T}{\partial x_3}\right] = \frac{\alpha}{\hbar_1\hbar_2\hbar_3}\left[\frac{\partial}{\partial x_1}\left(\frac{\hbar_2\hbar_3}{\hbar_1}\frac{\partial T}{\partial x_1}\right) + \frac{\partial}{\partial x_2}\left(\frac{\hbar_1\hbar_3}{\hbar_2}\frac{\partial T}{\partial x_2}\right) + \frac{\partial}{\partial x_3}\left(\frac{\hbar_1\hbar_2}{\hbar_3}\frac{\partial T}{\partial x_3}\right)\right] \tag{3}$$

where the parameters (scale factors, coordinates, and velocity components) for the FP, ICC, and sphere are given in Table 2. We further assume that viscous effects are confined to a thin hydrodynamic boundary layer δ, and that the flow is inviscid outside the boundary layer. One can neglect conduction in the x_2 direction by comparing it with conduction in the x_1 direction. Table 3 shows the comparison between the order of magnitude of these terms that have been evaluated by scaling analysis.

Table 2 Equivalent terms in curvilinear coordinates

	Scale factors			Coordinates			Velocity components		
System	$\hbar_1$	$\hbar_2$	$\hbar_3$	x_1	x_2	x_3	u_1	u_2	u_3
Cartesian	1	1	1	X	Y	Z	u	v	w
Cylindrical	1	r	1	r	θ	z	v_r	v_θ	v_z
Spherical	1	r	$r \sin\theta$	r	θ	ϕ	v_r	v_θ	v_ϕ

Table 3 Scaling analysis of the diffusive term for different body shapes

Body shape	$\frac{1}{\hbar_1\hbar_2\hbar_3}\frac{\partial}{\partial x_1}\left(\frac{\hbar_2\hbar_3}{\hbar_1}\frac{\partial T}{\partial x_1}\right)$	$\frac{1}{\hbar_1\hbar_2\hbar_3}\frac{\partial}{\partial x_2}\left(\frac{\hbar_2\hbar_3}{\hbar_2}\frac{\partial T}{\partial x_2}\right)$
FP	$1/\delta_T^2$	$1/L^2$
ICC	$1/\delta_T^2$	$4/(\theta D)^{2a}$
Sphere	$1/\delta_T^2$	$4/(\theta D)^{2a}$

[a]$\theta > 0$.

Furthermore, heat diffusion and convection in the x_3 direction can be neglected for the following reasons: the variations of the temperature along the x_3 direction for the FP and ICC are negligible; and assuming axisymmetry, one can neglect the temperature variation in the x_3 direction for the sphere.

The advection terms on the left side of Eq. (3) are approximated by a single equivalent term, i.e., $(\bar{v}_e/\hbar_2)(\partial T/\partial x_2)$, where $\bar{v}_e$ is the area-average effective velocity that will be determined later. This idea has been proposed by Oseen to linearize the inertia term for creeping flow, where Oseen assumed the convective term to be $V_\infty\nabla\cdot\boldsymbol{u}_i$ (for more details see Happel and Brenner[12]). In addition, the effective velocity has been introduced by Yovanovich et al.[1] and Jafarpur[13]; therefore, Eq. (3) becomes

$$\frac{\bar{v}_e}{\hbar_2}\frac{\partial T}{\partial x_2} = \frac{\alpha}{\hbar_1\hbar_2\hbar_3}\frac{\partial}{\partial x_1}\left(\frac{\hbar_2\hbar_3}{\hbar_1}\frac{\partial T}{\partial x_1}\right) \tag{4}$$

This equation is limited to the range $0 < x_2$, for the FP, and $0 \le x_2 \le \pi$, for the ICC and the sphere.

Equation (4) must be transformed to a transient heat conduction in order to find a suitable solution. Let us assume that the flow particles are moving with a constant velocity $\bar{v}_e$ around the body. Therefore, the particles will take time Δt to travel a distant $\hbar_2 x_2$. Furthermore, for $\Delta x_2 \to 0$ and $\Delta t \to 0$, one can define

$$\bar{v}_e = \hbar_2\frac{\partial x_2}{\partial t} \tag{5}$$

This concept was also used by Sideman[14] and Yovanovich et al.[1] Therefore, the energy equation can be transformed to the form of the transient heat conduction equation. Thus, by substituting Eq. (5) in Eq. (6), the energy equation can be written in the general form

$$\frac{\partial T^*}{\partial t} = \frac{\alpha}{\hbar_1\hbar_2\hbar_3}\left[\frac{\partial}{\partial x_1}\left(\frac{\hbar_2\hbar_3}{\hbar_1}\frac{\partial T^*}{\partial x_1}\right)\right] \tag{6}$$

where

$$x_1 \ge 0 \quad \text{for FP and} \quad x_1 \ge D/2 \quad \text{for ICC and sphere}$$

$$0 \le t \le \hbar_2\int_0^{x_2} dx_2/\bar{v}_e \quad \text{and} \quad T^* = \frac{T - T_\infty}{T_S - T_\infty}$$

The solutions of Eq. (6) from Carslaw and Jaeger[15] for the FP, ICC, and sphere, respectively, are as follows:

Flat plat solution

$$T^* = erfc(X/2\sqrt{\alpha t})$$

or

$$T^*|_{t=Y/\bar{v}_e} = erfc(X/2\sqrt{\alpha Y/\bar{v}_e}) \qquad Y > 0 \tag{7}$$

Infinite circular cylinder solution

$$T^* = \sqrt{D/(2r)}\, erfc\left(\frac{r - D/2}{2\sqrt{\alpha t}}\right) + \frac{(r - D/2)\sqrt{\alpha t}}{4r^{3/2}\sqrt{D/2}}\, ierfc\left(\frac{r - D/2}{2\sqrt{\alpha t}}\right) + \frac{(9D^2/4 - Dr - 7r^2)\alpha t}{32r^{5/2}(D/2)^{3/2}}\, i^2erfc\left(\frac{r - D/2}{2\sqrt{\alpha t}}\right)$$

This solution is valid for a short time. However, we are interested in the very short time solution, i.e., $t \to 0$, $Fo_D \ll 1$ ($Pe_D \gg 1$). Therefore, the first term of the above solution will be taken for this range, i.e.,

$$T^*|_{t=(\theta D)/(2\bar{v}_e)} = \sqrt{D/(2r)}\, erfc\left[\frac{r - D/2}{2\sqrt{(\alpha\theta D)/(2\bar{v}_e)}}\right] \qquad \theta > 0 \tag{8}$$

Sphere solution

$$T^* = \frac{D}{2}\frac{1}{r}\, erfc\left(\frac{r - D/2}{2\sqrt{\alpha t}}\right)$$

or

$$T^*|_{t=(\theta D)/(2\bar{v}_e)} = \frac{D}{2}\frac{1}{r}\, erfc\left[\frac{r - D/2}{2\sqrt{(\alpha\theta D)/(2\bar{v}_e)}}\right] \qquad \theta > 0 \tag{9}$$

The local wall heat flux that is related to the temperature gradient is

$$q_S(x_2) = -k(T_S - T_\infty)\frac{\partial T^*}{h_1 \partial x_1}\bigg|_{\text{surface}} \tag{10}$$

Taking the derivative of Eqs. (7–9) and substituting in Eq. (10) gives the local wall heat flux for three geometries:

$$q_S(Y) = k(T_S - T_\infty)\frac{1}{\sqrt{\pi}\sqrt{\alpha Y/\bar{v}_e}} \qquad \text{for FP} \tag{11}$$

$$q_S(\theta) = \frac{1}{\sqrt{\pi}}\frac{k(T_S - T_\infty)}{\sqrt{(\alpha D\theta)/(2\bar{v}_e)}} \qquad \text{for ICC} \tag{12}$$

$$q_S(\theta) = \frac{k(T_S - T_\infty)}{D/2} + \frac{1}{\sqrt{\pi}}\frac{k(T_S - T_\infty)}{\sqrt{(\alpha D\theta)/(2\bar{v}_e)}} \qquad \text{for sphere} \tag{13}$$

The transient conduction solution provides an analytic solution for the local Nusselt number, $\mathcal{L}q_S/k(T_S - T_\infty)$, which consists of the local boundary-layer term and the linear sum of this term and the constant term corresponding to the diffusive limit ($Re_D \to 0$) for the sphere only. Therefore, the area-averaged Nusselt number

$$Nu_{\mathcal{L}} = \frac{1}{A}\int\int_A \frac{\mathcal{L}q_S(x_2)}{k(T_S - T_\infty)}\, dA$$

is given by

$$Nu_{\mathcal{L}} = \frac{2}{\sqrt{\pi}}\sqrt{\frac{L\bar{v}_e}{\alpha}} \qquad \text{for FP}$$

$$Nu_D = \sqrt{\frac{2}{\pi}}\frac{2}{\sqrt{\pi}}\sqrt{\frac{D\bar{v}_e}{\alpha}} \qquad \text{for ICC}$$

$$Nu_D = 2 + \frac{1}{\sqrt{2.5}}\frac{2}{\sqrt{\pi}}\sqrt{\frac{D\bar{v}_e}{\alpha}} \qquad \text{for sphere} \tag{14}$$

The area-averaged effective velocity will be determined in the following sections.

Definition of $\bar{v}_e^\infty$ as $Pr \to \infty$

Table 4 shows step-by-step how one can determine $\bar{v}_e^\infty$ for the different body shapes when $Pr \to \infty$, $Re_{\mathcal{L}} \gg 1$ and $\delta \gg \delta_T$.

Definition of $\bar{v}_e^0$ as $Pr \to 0$

Let us consider that the body is immersed in an inviscid flow, i.e., $Pr \to 0$ and $Re_{\mathcal{L}} \gg 1$. Therefore, the thermal boundary layer (TBL), δ_T, around the body is very thick relative to the hydrodynamic boundary layer (HBL) δ. Therefore, at the edge of the TBL, we have the following relationships at the edge of the HBL:

$$v|_{(\delta + D/2)} = V_\infty \qquad \text{for FP}$$

$$v_\theta|_{(\delta + D/2)} = V_\infty \cdot \left\{1 + \left[\frac{D}{2(\delta + D/2)}\right]^3\right\}\sin\theta \qquad \text{for ICC}$$

$$v_\theta|_{(\delta + D/2)} = \frac{V_\infty}{2}\cdot\left\{2 + \left[\frac{D}{2(\delta + D/2)}\right]^3\right\}\sin\theta \qquad \text{for sphere} \tag{15}$$

In addition to the usual postulates, the HBL will be presumed to be thin relative to the radius of the cylinder or the sphere. Therefore, $v_\theta|_{\delta + D/2} = V = 2V_\infty \sin\theta$ (for ICC) and $1.5V_\infty \sin\theta$ (for sphere). Furthermore, the local velocity at arbitrary θ will be considered uniform across the TBL. The area-mean effective velocity is

$$\frac{\bar{v}_e^0}{V_\infty} = \frac{1}{A}\int\int_A \frac{V}{V_\infty}\, dA = C_0 \tag{16}$$

where $C_0 = 1$, 1.273, and 1.178 for the FP, ICC, and sphere, respectively.

Definition of $\bar{v}_e$ for all Pr

The method of Churchill and Usagi[16] "blending technique" will be used to develop a general expression for $\bar{v}_e$ valid for all Pr. The effective velocity can be determined in the following form based on the study of Refai Ahmed and Yovanovich[11]:

$$\bar{v}_e = \frac{\bar{v}_e^\infty}{[1 + (\bar{v}_e^\infty/\bar{v}_e^0)^n]^{1/n}} \tag{17}$$

Substituting $\bar{v}_e^0$ and $\bar{v}_e^\infty$ in Eq. (17) gives the effective velocity as a function of Prandtl number, power-law parameter γ, and blending parameter n

$$\frac{\bar{v}_e}{V_\infty} = \frac{C_0/[(2\gamma + 1)Pr^{1/3}]}{\{1 + [1/(2\gamma + 1)Pr^{1/3}]^n\}^{1/n}} \tag{18}$$

where $0 < \gamma < 1$ and $0 < Pr < \infty$. The values of n and γ will be determined in the following section.

Table 4 Definitions of $\bar{v}_e^\infty$ as $Pr \to \infty$ and $Re_{\mathscr{L}} >> 1$

Step	FP	ICC	Sphere
1. Continuity equation inside the HBL or TBL thicknesses	$\nabla \cdot \boldsymbol{u} = 0$		
2. Apply scaling analysis inside the HBL thickness	$u\|_\delta \sim V_\infty(\delta/L)$	$v_r\|_{\delta+D/2} \sim 2(\delta/D)\cdot[V(\theta)/\theta]$	
3. Applying scaling analysis inside the TBL thickness	$u\|_{\delta_T} \sim V_\infty(\delta_T^2/L\delta)$	$v_r\|_{\delta_T+D/2} \sim 2(\delta_T^2/D\delta)\cdot[V(\theta)/\theta]$	
4. Momentum equation inside the HBL thickness	$\nabla\cdot(\boldsymbol{u}_i u_2) = \delta_{i2}\nabla P + \nu\nabla^2 \boldsymbol{u}_2$		
5. Apply scaling analysis inside the TBL thickness	$(\delta/L) \sim \sqrt{1/Re_L}$	$(\delta/D) \sim \sqrt{\theta/2Re_D(\theta)}$	
6. Energy equation inside the TBL thickness	$\nabla\cdot(\boldsymbol{u}_i T) = \alpha\nabla^2\cdot T$		
7. Apply scaling analysis inside the TBL thickness	$(\delta/L) \sim (1/Pr^{1/3}\sqrt{Re_L})$	$(\delta/D) \sim (1/Pr^{1/3})\sqrt{\theta/2Re_D(\theta)}$	
8. Ratio of TBL to HBL thicknesses, δ_T/δ	$(V/V_\infty) \sim (\delta_T/\delta) \sim (1/Pr^{1/3})$	$[V/V(\theta)] \sim (\delta_T/\delta) \sim (1/Pr^{1/3})$	
9. Momentum flux inside TBL thickness	$\frac{\rho}{\delta_T}\int_0^{\delta_T} u_2(V - v_2)\,dx_1$		
10. Assume the flow has a uniform local effective velocity (function of θ for the ICC and sphere)	$\frac{\rho}{\delta_T}\int_0^{\delta_T} v_e^\infty(x_2)\cdot(V - v_2)\,dx_1$		
11. Equate steps 9 and 10, and rewrite it as a function of the momentum and displacement thicknesses	$\frac{v_e^\infty(x_2)}{V} = \frac{\delta_M^T}{\delta_D^T}$		
12. The last step can be expressed in the following form using scaling analysis	$v_e^\infty(x_2) = (V_\infty/Pr^{1/3})(\delta_M^T/\delta_D^T)$	$v_e^\infty(x_2) = (V(\theta)/Pr^{1/3})(\delta_M^T/\delta_D^T)$	
13. The velocity profile can be expressed in the power-law form	$(v/V) = (x_1/\delta_T)^\gamma$	$(v_\theta/V) = \{[x_1 - D/2)]/\delta_T\}^\gamma$	
14. Use similarity parameter, $\eta = y^n/\delta_T$ and integrate the velocity over the surface area. In addition the equations of $V(\theta)$ are obtained from the ideal flow solution, therefore, $\bar{v}_e^\infty$ are	$\frac{V_\infty}{(2\gamma+1)Pr^{1/3}}$	$\frac{1.273V_\infty}{(2\gamma+1)Pr^{1/3}}$	$\frac{1.178V_\infty}{(2\gamma+1)Pr^{1/3}}$

[a]$y = x_1 - D/2$ for ICC and sphere, $y = x_1$ for FP.

Results and Discussion

In order to determine the equation of Nu_J, one can substitute Eq. (18) into Eqs. (14), respectively. The area-averaged Nusselt number can be expressed in the following forms:

$$Nu_J = 1.128Re_L^{1/2}\frac{Pr^{1/3}/\sqrt{2\gamma+1}}{\left\{1 + \left[\frac{1.0}{(2\gamma+1)^3 Pr}\right]^{n/3}\right\}^{1/(2n)}} \quad \text{for FP}$$

$$Nu_D = 1.015Re_D^{1/2}\frac{Pr^{1/3}/\sqrt{2\gamma+1}}{\left\{1 + \left[\frac{1.0}{(2\gamma+1)^3 Pr}\right]^{n/3}\right\}^{1/(2n)}} \quad \text{for ICC}$$

$$Nu_D = 2 + 0.775Re_D^{1/2}\frac{Pr^{1/3}/\sqrt{2\gamma+1}}{\left\{1 + \left[\frac{1.0}{(2\gamma+1)^3 Pr}\right]^{n/3}\right\}^{1/(2n)}}$$

for sphere (19)

It has been found that $n = 3$ gives the best fit by matching Eqs. (19) with available air data.[11] In addition, it was found that simple correlations for γ as $F(Re_J)$ based on the previous works are given by

$$\gamma_L = \frac{1}{[1 + Re_L^{1.25}]^{1/5}} \quad \text{for FP}$$

$$\gamma_D = \frac{1}{[1 + (Re_D^{0.75}/300)^5]^{1/5}} \quad \text{for ICC}$$

$$\gamma_D = \frac{1}{[1 + Re_D^{1.25}]^{1/5}} \quad \text{for sphere} \qquad (20)$$

Flat Plate Model and Data Comparison

Figure 2 shows the relationship between $\{(Nu_J - Nu_J^0)/[F(Pr, \gamma_J)\sqrt{Re_J}]\}$ (Nu_J^0 for both the FP and ICC is 0) and Re_J. In addition, Fig. 2 shows the comparisons between the present model and the previous studies[4–6,8,9,14,17–29] for various Prandtl numbers.

Figure 2a shows the comparisons between the present approximate analytical solution [Eq. (19)], for the FP, and the previous analytical and experimental investigations. The analytical studies such as Pohlhausen[17] and Levy[18] are in a very good agreement with the present model at low Reynolds numbers. However, at high $Re_L = 10^4$, the maximum difference is within 30% ($Pr = 0.7$) and 35% ($Pr = 10$). On the other hand, the maximum difference between the present model and the Pohlhausen solution for $Pr = 0.01$ is found within 7%. In addition, it is found that the maximum difference between the present model [Eq. (19)], and the solutions of both Pohlhausen and Levy is 4%, if $\gamma = 1$, i.e., the velocity profile is linear across the thermal boundary layer.

Figure 2a also shows the comparisons between the experimental studies of Slegel and Hawkins[4] and Parmalee and Huebscher,[5] and the analytical solution[6] for high Re_L and the present model. It is interesting to observe from these comparisons that the Parmalee and Huebscher[5] data are below the Slegel and Hawkins[4] data by 40–50%. Furthermore, Knudsen and Katz[6] obtained agreement only with Slegel and Hawkins.[4]

Circular Cylinder Model and Data Comparison

Figure 2b shows the comparisons between the present model [Eq. (19)], for the ICC and the previous studies. One observes that the previous studies of Churchill and Bernstein,[8] Morgan,[9] King,[19] Kramers,[20] and Krall and Eckert[21] correlations are in a very good agreement with the present model, 5–7%,

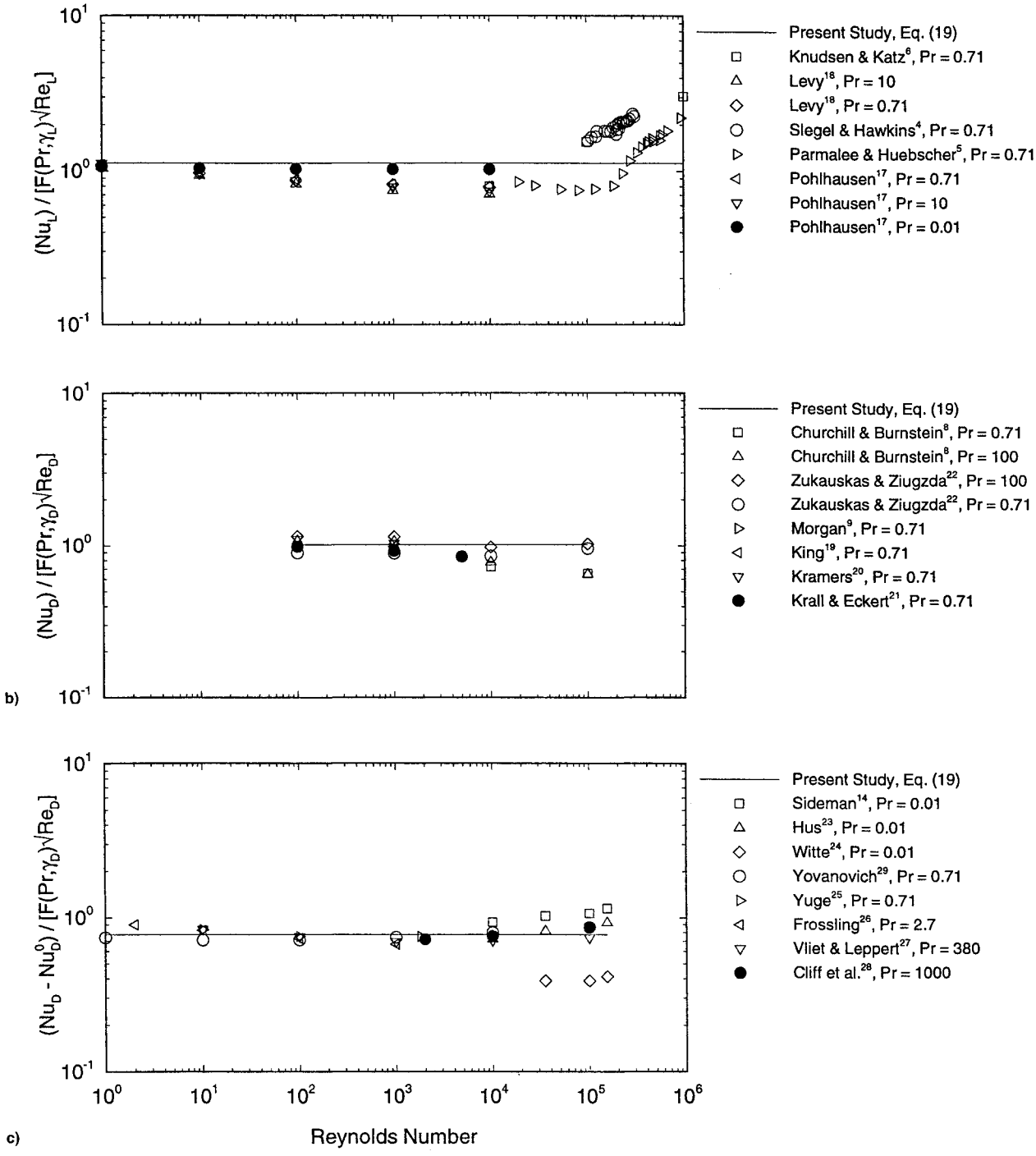

Fig. 2 Comparison between present approximate analytical model and previous studies for different Prandtl numbers: a) flat plate, b) infinite circular cylinder, and c) sphere.

in the range of Re_D from 10^2 to 10^3. In addition, the correlation of Zukauskas and Ziugzda[22] shows the same agreement with the present model at $Pr = 10^2$, but for $Pr = 0.71$ there is a difference of 12%. Furthermore, the study of Zukauskas and Ziugzda[22] is in very good agreement up to $Re_D = 10^5$ (maximum difference is 5%). The Churchill and Bernstein[8] correlation has a maximum difference of 35% with the present model at $Re_D = 10^5$. Achenbach[30] introduced experimental relationships between Nu_D and Re_D over the range $3 \times 10^4 < Re_D < 4 \times 10^6$, for $L/D = 1.36$. Achenbach[30] indicated that his experimental data were higher than Hilpert,[10] and this is due to blockage and low span ratio L/D effects in Hilpert.[10] Unfortunately, the present model cannot be compared against Achenbach,[30] where this model is valid up to $Re_D = 10^5$.

Sphere Model and Data Comparison

Figure 2c shows the comparisons between the present model [Eq. (19)], for the sphere and previous studies[4–6,8,9,14,17–29] for various Prandtl numbers. One observes that the maximum difference between the previous studies correlations and the present model in the range of $1 < Re_D < 10^5$ is approximately 11%, which generally occurs at $Re_D = 10^5$. On the other hand, there is almost a 33% difference between the present model and that of Sideman.[14] The main reason for this is that Sideman[14] approximated the convective term of the energy equation by assuming $(V_\infty/r)(\partial T/\partial\theta)$, and neglecting the curvature of the sphere with respect to the radial conduction. Achenbach[31] obtained experimental data up to $Re_D = 5 \times 10^6$ and he had good agreement with Yuge.[25] Therefore, the present investigation is also in agreement with Achenbach[31]

(where the present study has good agreement with Yuge[25] as shown in Fig. 2c).

Finally, one can conclude from Fig. 2 that the constant C_f for the flat plate, infinite circular cylinder, and sphere are 1.128, 1.015, and 0.775, respectively. In addition, $F(Pr, \gamma_f)$ has the general form

$$\frac{Pr^{1/3}}{[(2\gamma_f + 1)^3 + 1/Pr]^{1/6}}$$

for the FP, ICC, and sphere.

Design Correlations

The approximate analytical solutions are developed based on the scale length of L for FP and D for ICC. However, it is important to introduce a general solution for plates and circular cylinders. Therefore, Eq. (19) will be rewritten based on $\sqrt{A}$ as follows:

$$Nu_{\sqrt{A}} = 1.128(W/L)^{0.25}Re_{\sqrt{A}}^{0.5}F(Pr, \gamma_{\sqrt{A}}) \quad \text{FP} \quad (21a)$$

$$= 1.015(L/D)^{0.25}Re_{\sqrt{A}}^{0.5}F(Pr, \gamma_{\sqrt{A}}) \quad \text{ICC} \quad (21b)$$

$$= 3.545 + 1.032Re_{\sqrt{A}}^{0.5}F(Pr, \gamma_{\sqrt{A}}) \quad \text{sphere} \quad (21c)$$

The ratio of $(\sqrt{A}/D)$ is of order $\sqrt{(L/D)}$ as $L/D \to \infty$.

The equations of FP and ICC become functions of W/L and L/D, respectively. Therefore, the diffusive limit must be included in the solutions as follows:

$$Nu_{\sqrt{A}} = Nu^0_{\sqrt{A}} + 1.128(W/L)^{0.25}Re_{\sqrt{A}}^{0.5}F(Pr, \gamma_{\sqrt{A}})$$

$$\text{rectangular plate} \quad (22a)$$

$$= Nu^0_{\sqrt{A}} + 1.015(L/D)^{0.25}Re_{\sqrt{A}}^{0.5}F(Pr, \gamma_{\sqrt{A}})$$

$$\text{circular cylinder} \quad (22b)$$

The diffusive limits for circular cylinders and rectangular plates can be estimated, within $\pm 5\%$, as follows (more details in Ahmed[32] and Yovanovich[33]):

Circular cylinders

$$Nu^0_{\sqrt{A}} = 3.5(L/D)^{0.02} \qquad 0 < L/D \leq 1$$

$$= 3.385 + 0.082(L/D) \qquad 1 < L/D \leq 8 \quad (23)$$

$$= 4\sqrt{L/D}/\!/\, 2(L/D) \qquad 8 < L/D \quad (24)$$

Rectangular plates

$$Nu^0_{\sqrt{A}} = \frac{8.89\sqrt{W/L}}{/\!/\, 4W/L} \qquad 0.0 \leq L/W \leq 0.25$$

$$Nu^0_{\sqrt{A}} = \frac{(1.0 + \sqrt{L/W})^2}{\sqrt{0.5L/W}} \qquad 0.25 \leq L/W \leq 1 \quad (25)$$

Summary and Conclusions

A forced convection heat transfer method based on an approximate analytical approach is developed for simple body shapes such as the flat plate, infinite circular cylinder, and sphere. This method is valid for the range of Reynolds number, $0 < Re_f < 10^5$, and all values of the Prandtl number. In addition, the present method considers the effect of the velocity profile as a function of Reynolds number on the forced convection heat transfer. Also, this technique is shown to be in very good agreement with numerous previous investigations. Furthermore, $F(Pr, \gamma_f)$ was obtained in a general form that is valid for the FP, ICC, and sphere. Finally, this investigation has led to design correlations for circular cylinders and rectangular plates [Eq. (22)], which can be applied in a wide range of Reynolds number and all Prandtl numbers.

Acknowledgment

The authors acknowledge the financial support of the Natural Sciences and Engineering Research Council of Canada under Grant A7455.

References

[1]Yovanovich, M. M., Lee, S., and Gayowsky, T. J., "Approximate Analytical Solution of Laminar Forced Convection Heat from an Isothermal Plate," AIAA Paper 92-0248, 1992.

[2]Kays, W. M., and Crawford, M. E., *Convection Heat and Mass Transfer*, 2nd ed., McGraw–Hill, New York, 1980.

[3]Schlichting, H., *Boundary Layer Theory*, 6th ed., McGraw–Hill, New York, 1968.

[4]Slegel, L., and Hawkins, G., 1946; also see Ref. 6.

[5]Parmalee, G. V., and Huebscher, R. G., 1947; also see Ref. 6.

[6]Knudsen, J., and Katz, D., *Fluid Dynamics and Heat Transfer*, McGraw–Hill, New York, 1958.

[7]Ahmad, R. A., and Qureshi, Z. H., "Laminar Mixed Convection from a Uniform Heat Flux Cylinder," AIAA Paper 91-0383, 1991.

[8]Churchill, S. W., and Bernstein, M., "A Correlating Equation for Forced Convection from Gases and Liquids to a Circular Cylinder in Crossflow," *Journal of Heat Transfer*, Vol. 99, No. 2, 1977, pp. 300–306.

[9]Morgan, V. T., "The Overall Convection Heat Transfer from Smooth Circular Cylinders," *Advances in Heat Transfer*, Vol. 11, Academic, New York, 1975, pp. 199–264.

[10]Hilpert, R., 1933; also see Ref. 9.

[11]Ahmed, G. R., and Yovanovich, M. M., "Approximate Analytical Solution of Forced Convection Heat Transfer from Isothermal Spheres for all Prandtl Numbers," *Journal of Heat Transfer*, Vol. 116, No. 4, 1994, pp. 838–843.

[12]Happel, J., and Brenner, H., *Low Reynolds Number Hydrodynamics*, 2nd ed., Noordhoff International, Leyden, The Netherlands, 1973.

[13]Jafarpur, K., "Analytical and Experimental Study of Laminar Free Convection Heat Transfer from Isothermal Convex Bodies of Arbitrary Shapes," Ph.D. Dissertation, Dept. of Mechanical Engineering, Univ. of Waterloo, Waterloo, Ontario, Canada, 1992.

[14]Sideman, S., "The Equivalence of the Penetration Theory and Potential Flow Theories," *Industrial and Engineering Chemistry*, Vol. 58, No. 2, 1966, pp. 54–58.

[15]Carslaw, H. S., and Jaeger, J. C., *Conduction of Heat in Solids*, 2nd ed., Clarendon, Oxford, England, UK, 1959.

[16]Churchill, S. W., and Usagi, R., "A General Expression for the Correlation of Rates of Transfer and Other Phenomena," *AIChE Journal*, Vol. 18, 1972, pp. 1121–1132.

[17]Pohlhausen, E., 1921; see also Ref. 2.

[18]Levy, S., 1952; see also Ref 6.

[19]King, L., 1959; see also Ref. 9.

[20]Kramers, H., "Heat Transfer from Spheres to Flowing Media," *Physica*, Vol. 12, Nos. 2 and 3, 1946, pp. 61–81.

[21]Krall, K. M., and Eckert, E. R., "Local Heat Transfer Around a Cylinder at Low Reynolds Number," *Journal of Heat Transfer*, Vol. 95, No. 2, 1973, pp. 273–275.

[22]Zukauskas, A., and Ziugzda, J., *Heat Transfer of a Cylinder in Crossflow*, translated by E. Bagdonaite, edited by G. F. Hewitt, Hemisphere, Washington, DC, 1985.

[23]Hsu, S. T., *Engineering Heat Transfer*, D. Van Nostrand, New York, 1963.

[24]Witte, L. C., "An Experimental Study of Forced Convection Heat Transfer from a Sphere to Liquid Sodium," *Journal of Heat Transfer*, Vol. 90, 1968, pp. 9–12.

[25]Yuge, T., "Experiments on Heat Transfer from Spheres Including Combined Natural Convection," *Journal of Heat Transfer*, Vol. 82, 1960, pp. 214–220.

[26]Frössling, N. M., "The Evaporation of Falling Drops," *Gerlands Beitr. Geophys.*, Vol. 52, 1938, pp. 170–216.

[27]Vliet, G. C., and Leppert, G., "Forced Convection Heat Transfer from an Isothermal Sphere to Water," *Journal of Heat Transfer*, Vol. 83, 1961, pp. 163–175.

[28]Clift, R., Grace, J. R., and Weber, M. E., *Bubbles, Drops and Particles*, Academic, New York, 1978.

[29]Yovanovich, M. M., "General Expression for Forced Convection Heat and Mass Transfer from Isopotential Spheroids," AIAA Paper

88-0743, 1988.

[30]Achenbach, E., "Total and Local Heat Transfer from a Smooth Circular Cylinder in Cross-Flow at High Reynolds Number," *International Journal of Heat and Mass Transfer*, Vol. 18, 1975, pp. 1387–1395.

[31]Achenbach, E., "Heat Transfer from Spheres up to $Re = 6 \times 10^6$," *Sixth International Heat Transfer Conference*, Vol. 5, Toronto, Ontario, Canada, 1978, pp. 341–346.

[32]Refai Ahmed, G., "Experimental and Approximate Analytical Study of Forced Convection Heat Transfer from Isothermal Body Shapes," Ph.D. Dissertation, Dept. of Mechanical Engineering, Univ. of Waterloo, Waterloo, Ontario, Canada 1994.

[33]Yovanovich, M. M., "Dimensionless Shape Factors and Diffusion Lengths of Three-Dimensional Bodies," *Proceedings of the ASME/JSME Thermal Engineering Joint Conference*, Vol. 1, 1995, pp. 103–113.

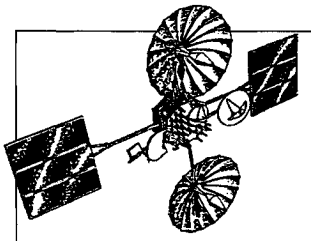

Satellite Thermal Control Handbook

David G. Gilmore, *editor*

The new *Satellite Thermal Control Handbook* (David G. Gilmore, Editor), published by The Aerospace Corporation Press and distributed by AIAA, is a compendium of corporate knowledge and heritage of thermal control of unmanned Earth-orbiting satellites. This practical handbook provides thermal engineers of all experience levels with enough background and specific information to begin conducting thermal analysis and to participate in the thermal design of satellite systems.

1994, 581 pp, illus, Paperback, ISBN 1-8849889-00-4, Order #: 00-4(945), AIAA Members: $59.95, Nonmembers: $79.95

Contents:

Satellite Systems Overview
Satellite Configurations
Orbits
Missions
Satellite Thermal Environments
Types of Environmental Loads
Environments in Typical Orbits
Launch/Ascent Environment
Thermal Design Examples
Spin-Stabilized Satellites
3-Axis-Stabilized Satellites
Propulsion Systems
Batteries
Antennas
Sun/Earth/Star Sensors
Cooled Devices
Solar Arrays
Systems Overview—The Hubble Space Telescope

Thermal Control Hardware
Section 1: Thermal Surface Finishes
Section 2: Mounting and Interfaces
Section 3: Multilayer Insulation and Barriers
Section 4: Heaters, Thermostats, and Solid State Controllers
Section 5: Louvers
Section 6: Radiators
Section 7: Thermoelectric Coolers
Section 8: PCMs and Heat Sinks
Section 9: Pumped Fluid Loops
Thermal Design Analysis
Satellite Project Phases
Thermal Design/Analysis Process Overview
Fundamentals of Thermal Modeling
Thermal Design Analysis Example-POAM
Margins
Thermal Math Model Computer Codes (SINDA)
Space Shuttle Integration
Engineering Compatibility
The Cargo Integration Review
Safety
Heat Pipes and Capillary Pumped Loops
Why a Heat Pipe Works
Constant-Conductance Heat Pipes
Diode Heat Pipes
Variable-Conductance Heat Pipes
Capillary Pumped Loops
Hybrid (Mechanically Assisted) Systems
Analysis
Materials
Compatibility
Testing
Heat Pipe Applications/Performance

Cryogenic Systems
Stored-Cryogen Cooling Systems
Cryogenic Radiators
Refrigerators
Design and Test Margins for Cryogenic Systems
Thermal Testing
Design Environments
Component Testing
Developmental and Subsystem Thermal Testing
Space Vehicle Thermal Tests
Factory and Launch-Site Thermal Testing
Test Techniques
Testing Checklist
One-of-a-Kind Spacecraft Thermal Testing
Technology Projections
Appendices

Place your order today! Call 1-800/682-AIAA

AIAA
American Institute of Aeronautics and Astronautics
Publications Customer Service, 9 Jay Gould Ct., P.O. Box 753, Waldorf, MD 20604
FAX 301/843-0159 Phone 1-800/682-2422 8 a.m. - 5 p.m. Eastern

Sales Tax: CA residents, 8.25%; DC, 6%. For shipping and handling add $4.75 for 1-4 books (call for rates for higher quantities). Orders under $100.00 must be prepaid. Foreign orders must be prepaid and include a $25.00 postal surcharge. Please allow 4 weeks for delivery. Prices are subject to change without notice. Returns will be accepted within 30 days. Non-U.S. residents are responsible for payment of any taxes required by their government.